

NATURAL RADIO SOURCE AND SPACECRAFT SIGNAL MEASUREMENTS  
AT **Ka-BAND (32.0 GHz)** AND X-BAND (8.4 GHz)  
USING A 34-METER BEAM-WAVEGUIDE ANTENNA

David D. Morabito  
Jet Propulsion Laboratory  
California Institute of Technology  
Phone: 818-354-2424, E-mail: david.d.morabito@jpl.nasa.gov

## 1. INTRODUCTION

NASA's Deep Space Network (DSN) Technology Program at the Jet Propulsion Laboratory (JPL) is evaluating the use of the **Ka-band** frequency allocation band (31.8 GHz to 32.3 GHz) for deep space to earth telecommunications. During the early years of deep space missions, from 1959 through 1964, 960 MHz was the frequency used for deep space to earth telecommunications. S-band (2290 MHz to 2300 MHz) was used as the primary link frequency band from 1965 to 1977. X-band (8400 MHz to 8450 MHz) became the principal operational deep space to earth link frequency band in 1977, beginning with the Voyagers, and continuing to the present time (Ref. 1).

**Ka-band** provides an advantage 11.6 dB (ratio of 14.5) over X-band in the effective isotropic radiated power (EIRP) transmitted from a spacecraft with the same transmitter output power level and the same antenna size. The advantage comes from the increased antenna gain and narrower beamwidth that occurs due to the shorter wavelength. The higher **Ka-band** EIRP can be used to allow for a higher data rate which allows for increased data volume or decreased transmission time. The **Ka-band** advantage can also be used to maintain the same data rate used at X-band, while decreasing the spacecraft transmitter power, antenna size, or to allow for the use of smaller diameter receiving antennas. The **Ka-band** link advantage over X-band is reduced from the ideal EIRP advantage of 11.6 dB to a net link advantage of 6 dB to 8 dB by atmospheric loss and noise that are higher than at X-band and DSN antenna efficiency that is lower than at X-band. Increased weather susceptibility at **Ka-band** must also be taken into consideration.

A telecommunications deep space **Ka-Band** Link Experiment (**KaBLE**) was conducted to confirm and refine the study results, and to help understand any obstacles that might affect the use of **Ka-band**. **KaBLE** was part of the Mars Observer (MO) mission. The signals emitted by MO were tracked by the DSN's Research and Development (R&D) 34-meter beam-waveguide (BWG) antenna at DSS-13, located in the DSN's Goldstone Complex in California. DSS-13 tracked the **Ka-band** signal at 33.7 GHz and the X-band signal at 8.42 GHz to compare the performance of the two links between January and August, 1993. The loss of MO in 1993 caused a change in plans for the continuation of the comparative study.

The **Ka-band** Antenna Performance Experiment Project (**KaAP**) was initiated in December 1993 to evaluate antenna efficiency by observing natural radio sources at both X-band and **Ka-band**. The observations allow the antenna efficiency and weather effects at each frequency band to be measured as performance improvements and configuration changes are made at the ground station. DSS-13's performance at **Ka-band** and X-band are quantified using the antenna efficiency data and system operating noise temperature (Top) data from both bands.

Knowledge quantifying the temporal variability of the **Ka-band** link performance due to weather effects can help planners of future flight projects develop operational strategies for the use of **Ka-band** that are robust, efficient and optimal. Two spacecraft with **Ka-band** transmitters are expected to be employed in the continuation of the **Ka-band** and X-band link studies. **SURFSAT-1**, launched on November 4, 1995, is a DSN Technology Program earth-orbiting flight experiment. **SURFSAT-1** **Ka-band** and X-band data are currently being acquired and analyzed for the purpose of characterizing the link advantage. Mars Global Surveyor (**MGs**), scheduled for launch in November 1996, will carry **KaBLE-II**, another DSN Technology Program experiment.

This paper addresses the three current **Ka-band** and X-band activities, 1) **KaAP**, 2) **SURFSAT-1**, and 3) **KaBLE-II**'s upcoming **Ka-band** experiments aboard Mars Global Surveyor.

## 2. KaAP: OBSERVATIONS USING NATURAL RADIO SOURCES

This **section** addresses the analysis of KaAP antenna efficiency measurements acquired at DSS-13. For detailed descriptions of the ground station and antenna configuration, the measurement technique, and the modeling used in the data processing, the reader is referred to Ref. 2. The radiation from natural **wideband-noise** radio sources incident on DSS-13's main reflector, **subreflector** and beam-waveguide **mirrors** is channeled into a subterranean pedestal room to two feed-horn/low-noise-amplifier (LNA) packages, one at 8.425-GHz (X-band) and one at **32.0-GHz (Ka-band)**. The signals are downconverted, filtered, and recorded for later processing.

The observations of the radio sources at Ka-band and X-band are processed and converted into estimates of the antenna efficiency at each frequency. Each pass or experiment **consists** of a series of radio source **observations** distributed over different parts of the sky over a wide elevation angle range. There are typically one to two tracks per month, with each lasting 8 to 24 hours in duration. Each track consists of 1) a series of boresight observations of different radio sources, 2) a series of radiometer calibrations, and 3) tipping curves used to estimate the effect of the atmosphere. The **boresight** observations alternate with the calibrations during the main body of the pass, with tipping curves usually performed at **the** start or end of the pass.

The boresight observations are conducted to evaluate antenna efficiency. Each boresight observation of a radio source involves stepping the antenna beam across the source while taking **lop** measurements using a Total Power Radiometer (**TPR**). The peak noise temperature due to the source is estimated from a fit of a linearized Gaussian beam model **over** the Top measurements in two orthogonal directions across the radio source. The peak source noise temperatures are converted into estimates of antenna efficiency using the radio source's flux density, and correction for the angular flux **distribution** over the antenna beam, atmospheric attenuation (to refer the measurements to **zero** atmosphere), and any system non-linearity which may be present.

The radiometer calibrations are **routinely** conducted to correct for gain changes, and allow any system non-linearity (typically less than 0.5%) to be determined (Ref. 3).

The tip curve observations are performed to determine 1) the atmospheric **loss** factor used to refer the antenna efficiency measurements to **zero** atmosphere, and 2) the atmospheric noise temperature used for statistical cross-comparisons with independent Water Vapor Radiometer (**WVR**) and surface model estimates. **Each** 30-minute **tip** curve consists of a set of cold-sky Top measurements at elevation angles which span from near horizon to zenith.

Since the KaAP data acquisition began in December 1993 after the end of the **KaBLE** experiment, the measurements were acquired on a routine basis. Each time a configuration change was implemented, the performance determined from the new set of measurements was compared with that of the previous configuration.

The antenna efficiency measurements gathered from different radio **sources**, and different observing sessions for a given frequency band, and station configuration are combined **into** a common data set. An antenna efficiency versus elevation angle curve is least-squares **fit** to the data using a 2nd-degree polynomial model. Fig. 1 displays the measured efficiencies, estimates of error bars, and the best-fit polynomial curves versus elevation angle for X-band and **K<sub>a</sub>-band** data acquired from February to November 1995.

The measured **X<sup>a</sup>-band** peak antenna efficiency is 71.1% at 37 deg elevation. The rms error of the X-band data points about the best-fit curve is 0.9% over 77 observations. The measured Ka-band peak antenna efficiency is 57.1% at 40.8 deg elevation. The rms error of the Ka-band data about the **best-fit** curve is 1.9% over 444 observations. The measured peak efficiencies are in agreement with **predicted** values based on estimates of individual **contributors** (Ref. 2).

Most anomalous Ka-band data points were automatically **removed from the data** set when the boresight derived pointing corrections exceeded a set 2 **millideg** tolerance. The remaining anomalous data points were found to be **correlated** during periods when 1) the measured wind speeds exceeded 20 mph and the antenna was pointed directly into the direction of the oncoming wind, 2) the wind speed exceeded 30 mph, 3) significant gain fluctuations occurred, or 4) especially turbulent weather conditions occurred, thus degrading the boresight technique. These points were subsequently removed from the data set.

The rms scatter of the data about the fitted polynomial curves (Fig. 1) provides a measure of the noise in the data. The major contributors to this scatter are radiometer gain instability, atmospheric noise variations, and error in determination of the atmospheric loss factors used to refer the measurements to zero atmosphere. Errors due to misprinting are estimated to be small and are below 0.5%.

Absolute errors due to uncertainty in the flux densities of the radio sources are about 3%.

The antenna gain (estimated from the antenna efficiencies) divided by system operating noise temperature,  $G/T_{op}$ , figure-of-merit, characterizes the ground station contribution used in link studies by spacecraft mission planners. Fig. 2 displays the  $G/T_{op}$  estimated from the data at both frequencies. The relative link advantage of Ka-band over X-band plotted in Fig. 3 is the Ka-band  $G/T_{op}$  data point in Fig. 2 difference from the fit value over the X-band data points. A 7 to 9 dB advantage of Ka-band relative to X-band is apparent upon inspection of Fig. 3. However, if both Ka-band and X-band  $G/T_{op}$  measurements are adjusted for projected noise temperatures of improved future LNA's, the resulting link advantage will lie between 6 to 8 dB.

Also shown in Figs. 2-3 are the 10%, 50%, and 90% weather curves derived from independent Water Vapor Radiometer (WVR) statistics (Ref. 4). Because of the small spread between these curves at X-band, only one curve is shown in Fig. 2 for X-band. Upon a close examination of the distribution of data points about these curves, it is apparent that 1) there are less data acquired during turbulent weather conditions due to the boresight technique breaking down under these conditions, and 2) the number of observations which lie above the 10% curve is higher than expected (23%). This is partially due to the selection effect noted in (1). After making a correction for this effect, the resulting 16% is still high but consistent with the known absolute uncertainty of the data. As more data are gathered, improved understanding of atmospheric effects at Ka-band will result from this effort.

### 3. OBSERVATIONS USING SPACECRAFT SIGNALS: SURFSAT-1

The SURFSAT-1 project was originally conceived in December 1986 as a very simple inexpensive experiment package carried as a secondary payload aboard a Delta II rocket. A major programmatic objective of SURFSAT-1 was to provide hands-on experience in spacecraft design and fabrication to college students from Caltech's Summer Undergraduate Research Fellowship (SURF) program. The work of building the spacecraft was initiated in the summer of 1987 by SURF students with the assistance of JPL engineers. Since then, more than 60 students have worked on SURFSAT-1.

SURFSAT-1 is the test vehicle for an X/Ka link experiment as well as Space Very Long Baseline Interferometry (SVLBI) experiments. The X/Ka link experiment uses X-band (8.478 GHz) and Ka-band (32.03 GHz) signals transmitted from SURFSAT-1 in order to assess the Ka-band gain advantage over X-band. The SVLBI experiments are conducted to test a new set of n-m DSN ground stations being built to provide support for upcoming international spacecraft, Russia's RADIOASTRON at X-band and Japan's VSOP at Ku-band (14 GHz).

SURFSAT-1, the secondary payload to the RADARSAT satellite, was launched on November 4, 1995 aboard a Delta II 7920 launch vehicle. After separation from RADARSAT, SURFSAT-1 was placed into a 936 km altitude by 1494 km altitude Sun-synchronous orbit with an intended gravity gradient stabilized orientation (nose nadir-pointed and not spinning). Its orbital period is about 1.5 hours. SURFSAT-1 was commanded on and its signal initially acquired over Goldstone during its third orbit at DSS-13.

SURFSAT-1, a passive satellite with no maneuver or telemetry capability, consists of two solar-powered aluminum boxes harnessed to the second stage of the Delta II launch vehicle. Within the two boxes are transponders used to generate the desired milliwatt level signals (X-band and Ka-band for the X/Ka box and Ku-band for the Ku box). The boxes also carry electronics that receive commands from the ground station to switch operational states and provide regulated power input from the solar panels mounted on the outside of each box. Cylindrical waveguide antennas located on corners of each box provide overlapping hemispherical coverage at all three frequencies. One box contains the X-band and Ka-band antennas mounted on opposite earth-facing corners. The other box contains a Ku-band antenna mounted on one corner used for SVLBI experiments. The X-band and Ka-band antennas radiate simultaneously at their

respective frequencies during periods when that box is commanded on for the X/Ka link experiment.

The intended goal of the X/Ka-band experiment is to quantify the performance gain of **Ka-band** over X-band to a 0.-5 dB accuracy. The experiment was intended to produce an accumulated database of X and Ka-band signal strengths and resulting link advantage over diverse weather conditions. Initial challenges to realizing this goal included 1) having pointing predict capability of sufficient accuracy to initially point the ground antenna well within the X-band beam, and 2) implementing a form of autotracking to correct the ground station pointing using the Ka-band signal. The first challenge was initially realized by generating predicts from specially requested Space Command orbital elements. Later, two-way Doppler data using **DSS-13's** transmitter and **SURFSAT-1's** transponders produced highly accurate orbit solutions which were used to generate pointing predicts to 10 millideg accuracy. The second challenge was realized by implementing a form of autotracking which moves one of the BWG mirrors. The **DSS-13** beam is scanned in a circle about its predicted on-point center, and the amplitude information is used to provide corrections to the true peak of the antenna beam. These corrections are then used to adjust the pointing of the main reflector to about 3 millideg accuracy.

**SURFSAT-1** data acquisition and analysis activities started shortly after launch. Between November 1995 and May 1996, a total of 161 tracking passes were conducted at **DSS-13** and their signal strengths analyzed. The ground station antenna tracks **SURFSAT-1** as it moves across the sky during a pass. Signal strength data are obtained from two Hewlett.-Packard Spectrum Analyzers (**HPSA**). The received frequencies from the Electronic Tone Tracker (**ETT**) are converted to **Surfsat-1's** temperature which in turn are used in the signal strength model. Ground station Top measurements are obtained from the **TPR**. **Autotrack** derived angle data from the antenna's pointing system and the predicted pointing angles and range from Navigation are also utilized in the analysis processing.

The received signal strengths are compared to a model which assumes a specific orientation of the satellite as it moves across the sky. Included in the model are 1) a temperature dependent transmitted signal power signature using the **ETT frequency data and pre-flight curves**, 2) the **SURFSAT-1** antenna patterns at the satellite's assumed orientation, 3) the space loss correction, 4) the atmospheric attenuation, and 5) the ground station gain.

After the initial challenges discussed above were met, the analysis showed that the expected orientation model (roll-axis is nadir pointed and the X/Ka box is facing into the direction of motion of the spacecraft) did not fit the data. The model was upgraded to account for three degrees of freedom of **Surfsat-1's** orientation, 1) rotation of satellite about roll axis, 2) rotation of roll axis vector from nadir-point, and 3) rotation (of roll axis' projection in plane perpendicular to nadir direction) from velocity direction vector. In addition, an improved Ka-band antenna pattern model was derived from **pre-flight** antenna pattern measurements.

After these upgrades were implemented, it was found that for single passes with sufficient SNR, the data could be fit by one (or more) orientation models quite well. However, it was found that the single-pass derived models did not fit the data from adjacent passes implying that the orientation is changing significantly.

The next challenges in the data analysis are resolving ambiguities between different "optimum" models over single passes and identifying the time varying signature of the orientation angles between passes. The interpretation and identification of the time varying signature of the orientation angles over multiple passes is difficult due to sparseness in the data sampling. This is because 1) **SURFSAT-1** is visible only during 4 to 5 orbits per day with sufficient duration, each track lasting only 10 to 20 minutes, 2) on the average only about 6 passes per week are tracked, 3) in order to do orbit determination with desired accuracy (required for pointing predicts), much of the data are taken in two-way mode (two-way frequency data are coherent with the ground uplink and hence do not contain satellite temperature information required in the signal strength model), and 4) because of **SURFSAT-1's** rocking and rolling motion, much of the time the satellite is in unfavorable orientations to yield a sufficient quantity of data with sufficient signal strengths at both bands.

Figs. 4 and 5 display the received signal strength and one "best-fit"

model for X-band and **Ka-band**, respectively. These data were acquired during a track on May 6, 1996 when **SURFSAT-1's** antennas were favorably oriented with respect to the station. The orientation model plotted is not the only one which fits the small arc of data this well. It is anticipated that as more data from future passes (and other tracking sites) are acquired and analyzed and the rocking and rolling motion stabilizes (hopefully), orientation model ambiguities can be resolved and a unique time-dependent orientation model will result from further analysis. The prime mission is expected to last until March 1996 when **MGS KaBLE-II** is expected to start generating useful X/Ka data.

#### 4. FUTURE OBSERVATIONS USING SPACECRAFT SIGNALS: **KaBLE-II**

Another spacecraft with **Ka-band** capability, Mars Global Surveyor (**MGS**) is planned for a November 1996 launch. **MGS** carries **KaBLE-II**, the continuation of the Mars Observer (**MO**) **KaBLE** experiment which ended in **August** 1993. X-band and **Ka-band** signals will be received at **DSS-13**. The goals for **KaBLE-II** will include data acquisition for the **DSN's Ka-band** systems planning and demonstration. The **DSN Ka-band** implementations for **Cassini** and New Millennium can be tested with **KaBLE-II's** signals. During the ongoing data acquisition, signal strength data at both X-band and **Ka-band** will be gathered under a wide variety of weather conditions to quantify the X/Ka link advantage.

Among **KaBLE-II's** objectives will be acquisition of 2 kbps **Ka-band** telemetry, Doppler and range data from a deep space link. The relative performance of X and **Ka-band** telemetry over an extended period will be quantified including during periods when **MGS** is angularly near the sun. Because **Ka-band** signals pass more easily through the Sun's corona than do X-band signals, **Ka-band** communications should be more easily maintained during solar conjunction. This is one expected advantage of **Ka-band**. Year round statistics will be collected on signal amplitude, phase, frequency and SNR fluctuations as a function of station and atmospheric parameters. Range data will also be acquired and analyzed at both bands as well as dual-frequency ranging to quantify ranging performance. During superior conjunction in May 1998, the unmodulated carrier using the Ultra-Stable Oscillator (**USO**) will be used to gather statistics of the phase variations versus solar elongation angle.

The **KaBLE-II** experiment on **MGS** represents a significant step beyond the **MO KaBLE** experiment. The **Ka-band** signal will be stronger for two reasons. **MGS** will have higher transmitter power at **Ka-band** (1W versus 25 mW) and the **Ka-band** signal will be fully illuminated by the 1.5 m High Gain Antenna (**HGA**) (**KaBLE** used the back side of the 28 cm subreflector to the **HGA** as the **Ka-band** antenna). Also the **Ka-band** signal frequency will be in the desired 32 GHz **Ka-band** region rather than the 33.7 GHz used for **MO KaBLE**.

#### 5. CONCLUSION

The **KaAP** antenna efficiency measurement analysis and preliminary **SURFSAT-1** signal-strength measurement analysis using the **DSS-13 R&D beam waveguide (BWG)** antenna have been discussed. Also a description of the upcoming **KaBLE-II** experiment aboard Mars Global Surveyor was presented. These ongoing efforts will add useful data for characterizing the link advantage of **K<sub>a</sub>-band** over X-band.

#### ACKNOWLEDGEMENTS :

I would like to thank C. Stelzried (who initiated the **KaAP** effort) and c. Edwards for their support, guidance and continuing interest in this work; R. Clauss (**SURFSAT-1** PI) for his comprehensive review and historical perspective reflected in the introduction; M. Tinto and S. Butman (**KaBLE-II** P) for their review comments; the **DSS-13** station personnel for conducting the experiments (G. Bury, J. Crook, G. Farner, J. Garnica, C. Goodson, R. Littlefair, R. Reese, and L. Smith); L. Skjerve and L. Tanida for development and operation of the **HPSAs**; T. Rebold for assistance in data analysis and software development; J. Border for Electronic Tone Tracker support; M. Gatti and J. McCluskey for scheduling the tracks; and M. Ryne for navigation support. The support of Utah State University and GlobeSat in Logan, Utah for teaching small satellite technology to the first group of **SURFSAT** students and the **SURFSAT** sponsors during the summer of 1987 is also acknowledged. This paper presents the results of one phase of research carried out at the Jet Propulsion Laboratory, California Institute of Technology, under contract with the National Aeronautics and Space Administration.

**REFERENCES:**

- 1) Corliss, W. R., "History of the Deep Space Network", May 1, 1976, NASA Report No. CR-151915.
- 2) D. D. Morabito "The Efficiency Characterization of the DSS-13 34-Meter Beam-Waveguide Antenna at Ka-band (32.0 and 33.7 GHz) and X-band (8.4 GHz)", The Telecommunications and Data Acquisition Progress Report 42-125, vol. January - March 1996, Jet Propulsion Laboratory, Pasadena, California, May 15, 1996.
- 3) c. T. Stelzried, and M. J. Klein, "Precision DSN Radiometer Systems: Impact on Microwave Calibrations", Proc. of the IEEE, vol. 82, pp. 776-787, May 1994.
- 4) L. J. Harcke, F. F. Yi, M. K. Sue, and H. H. Tan, "Recent Ka-Band Weather Statistics for Goldstone and Madrid", The Telecommunications and Data Acquisition Progress Report 42-125, vol. January - March 1996, Jet Propulsion Laboratory, Pasadena, California, May 15, 1996.

Fig. 2 G/T Link Performance

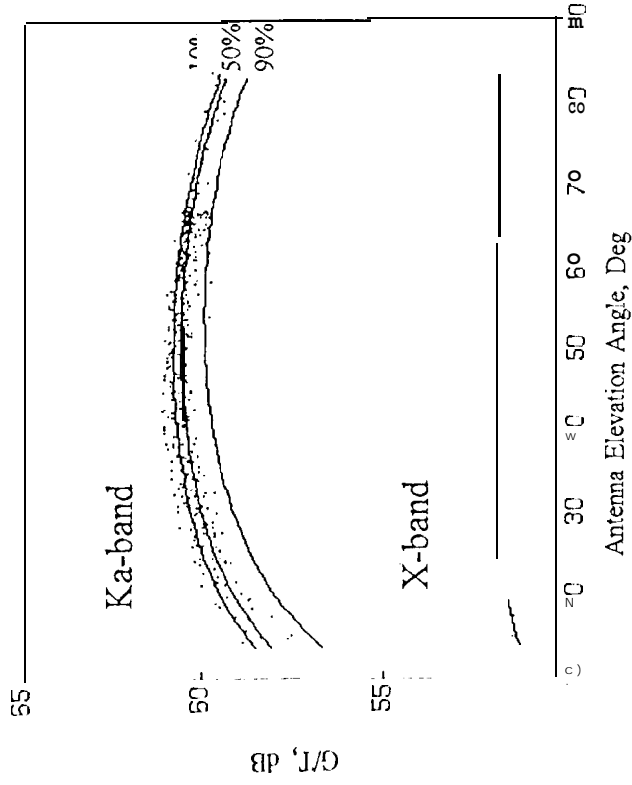


Fig. 3 G/T Link Advantage

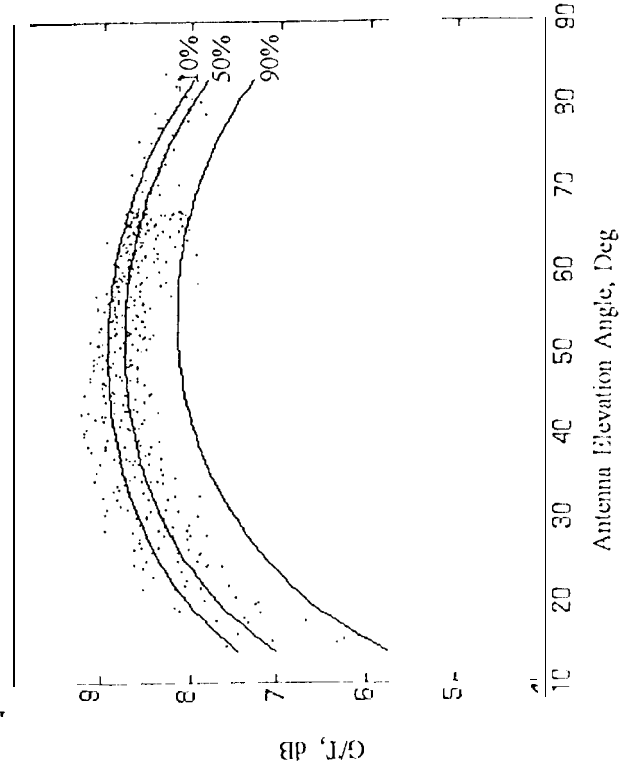


Fig. 1 Antenna Efficiency

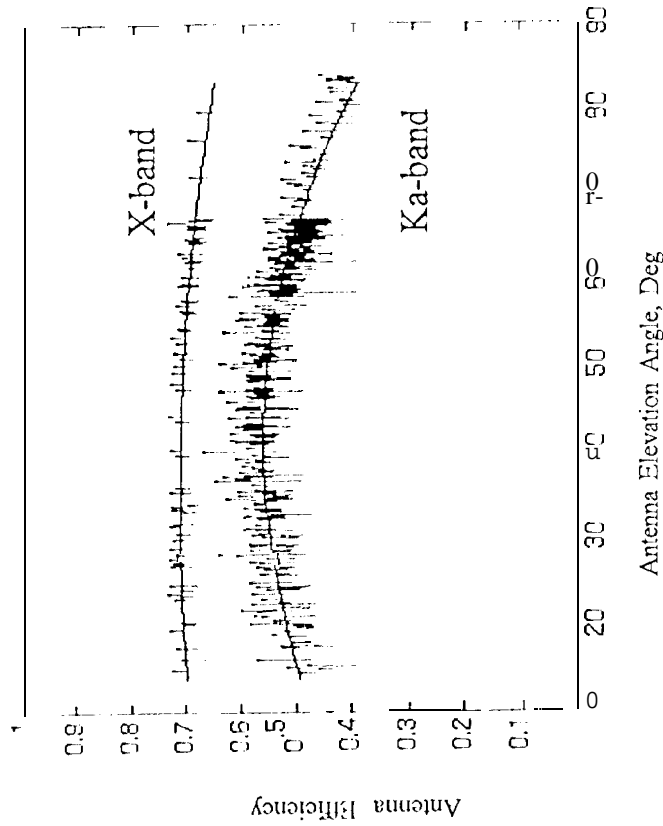


Fig. 4 SURFSAT-1 X-Band (8.5 GHz)

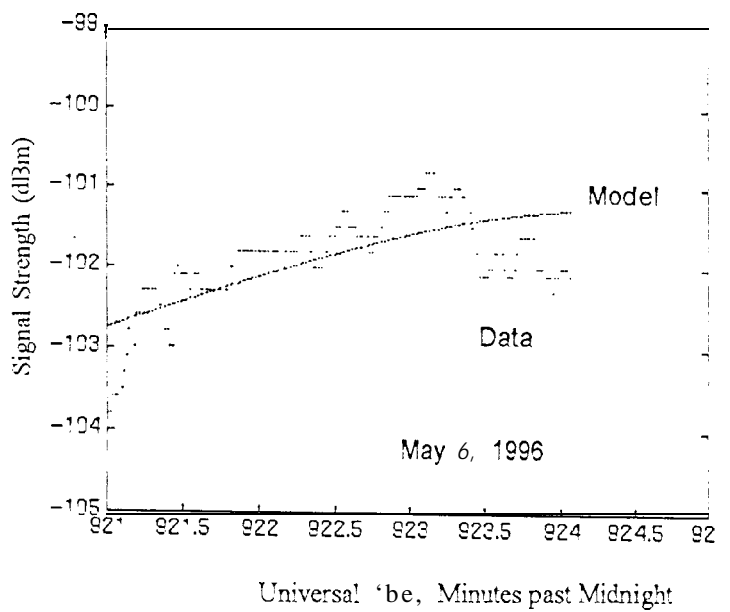


Fig. 5 SURFSAT-1 Ka-Band (32.0 GHz)

